

# A model-independent test of pre-recombination New Physics: Machine Learning based estimate of the Sound Horizon from Gravitational Wave Standard Sirens and the Baryon Acoustic Oscillation Angular Scale

William Giarè,<sup>1,\*</sup> Jonathan Betts,<sup>1,†</sup> Carsten van de Bruck,<sup>1,‡</sup> and Eleonora Di Valentino<sup>1,§</sup>

<sup>1</sup>*School of Mathematics and Statistics, University of Sheffield,  
Hounsfield Road, Sheffield S3 7RH, United Kingdom*

In any cosmological model where spacetime is described by a pseudo-Riemannian manifold, photons propagate along null geodesics, and their number is conserved, upcoming Gravitational Wave (GW) observations can be combined with measurements of the Baryon Acoustic Oscillation (BAO) angular scale to provide model-independent estimates of the sound horizon at the baryon-drag epoch. By focusing on the accuracy expected from forthcoming surveys such as LISA GW standard sirens and DESI or Euclid angular BAO measurements, we forecast a relative precision of  $\sigma_{r_d}/r_d \sim 1.5\%$  within the redshift range  $z \lesssim 1$ . This approach will offer a unique model-independent measure of a fundamental scale characterizing the early universe, which is competitive with model-dependent values inferred within specific theoretical frameworks. These measurements can serve as a consistency test for  $\Lambda$ CDM, potentially clarifying the nature of the Hubble tension and confirming or ruling out new physics prior to recombination with a statistical significance of  $\sim 4\sigma$ .

## I. INTRODUCTION

The disparity between the present-day expansion rate of the Universe – quantified by the Hubble parameter  $H_0$  – as determined by the SH0ES collaboration using Type-Ia supernovae ( $H_0 = 73 \pm 1$  km/s/Mpc) [1–3], and inferred by the Planck Collaboration from measurements of the Cosmic Microwave Background (CMB) temperature and polarization anisotropies angular power spectra, assuming a standard  $\Lambda$ CDM model of cosmology ( $67.04 \pm 0.5$  km/s/Mpc) [4], has been regarded with significant attention by the cosmology community.

Barring any potential systematic origin of the discrepancy,<sup>1</sup> the Hubble tension might well stand as compelling evidence for the necessity of new physics beyond  $\Lambda$ CDM. While not aiming to offer a comprehensive overview of the debate that has heated up the community in the past few years,<sup>2</sup> it is fair to say that attempts to tackle this issue have predominantly clustered around two distinct approaches: early-time and late-time solutions. Broadly speaking, the former category entails proposals suggesting new physics acting prior to recombination, while the latter comprises models that seek to modify the expansion history of the Universe after recombination.

This dichotomy in approach stems from the highly precisely determined angular scale of the acoustic peaks in the CMB spectra,  $\theta_s$  [4], which sets the ratio between the

sound horizon at recombination  $r_s(z_*)$  and the angular diameter distance to the last scattering surface  $D_A(z_*)$ . Increasing the value of  $H_0$  without disrupting the acoustic scale requires either a reduction in the value of the sound horizon – a core tenet of early-time solutions – or a distinct post-recombination expansion history of the Universe capable of compensating for a higher  $H_0$  while preserving the angular diameter distance to the last scattering surface [14].

Despite the apparent simplicity of the goals characterizing these two approaches, neither has proven effective in resolving the  $H_0$ -tension thus far, leaving the problem widely open. The primary challenge in the current landscape of solutions lies in the fact that both early and late-time observations tightly constrain new physics at their respective cosmic epochs, posing significant hurdles for model-building. Early-time solutions typically act near the last scattering surface, a cosmic epoch severely constrained by CMB measurements. Consequently, a common issue with early-time solutions is the need for a moderate level of fine-tuning to maintain a good fit to the CMB data, making it difficult to increase  $H_0$  enough to match the SH0ES results [15–17].<sup>3</sup> On the other hand, late-time solutions are well constrained by observations of the local Universe, such as Baryon Acoustic Oscillations (BAO) and Supernovae (SN), which generally favor a  $\Lambda$ CDM-like cosmology at low redshifts [18–21].<sup>4</sup>

Given the difficulties in constructing successful models, it seems natural to step back and consider independent

---

\* [w.giare@sheffield.ac.uk](mailto:w.giare@sheffield.ac.uk)

† [jbetts3@sheffield.ac.uk](mailto:jbetts3@sheffield.ac.uk)

‡ [c.vandebruck@sheffield.ac.uk](mailto:c.vandebruck@sheffield.ac.uk)

§ [e.divalentino@sheffield.ac.uk](mailto:e.divalentino@sheffield.ac.uk)

<sup>1</sup> This scenario appears less likely following the extensive review conducted by the SH0ES collaboration, where several potential sources of systematics have been examined [1, 5, 6].

<sup>2</sup> We refer to Refs. [7–13] for recent reviews on the Hubble tension problem, the related proposed solutions and their possible implications.

---

<sup>3</sup> In Ref. [16], seven hints were proposed, suggesting that a compelling definitive solution might entail combining early and late-time new physics.

<sup>4</sup> Recent BAO measurements released by the DESI collaboration [22–24] seem to suggest dynamical dark energy, potentially reopening the avenue for new physical mechanisms at late times that could address the Hubble tension [25]. See also Refs. [26–31] for discussions.

methods to test signals of new physics without relying on any particular framework. For late-time new physics, this is typically achieved through model-independent reconstructions of available datasets using Machine Learning (ML) techniques such as Artificial Neural Networks (ANN) or Gaussian Processes (GP). These approaches significantly limit theoretical assumptions in data analysis. Conversely, the state-of-the-art observational constraints on the early universe – particularly at the time of recombination – are largely dependent on the cosmological model assumed to analyze Planck CMB measurements. Therefore, a robust assessment of a fundamental physical quantity characterizing the early universe, not contingent on specific models, will certainly represent an important step forward for testing new physics before recombination and clarifying, once and for all, the intricate debate surrounding early and late-time solutions.

In this work, we demonstrate that geometric distance measurements in the local Universe can be used to independently measure the sound horizon. By using forecast measurements of Gravitational Waves (GWs) standard sirens from future surveys such as LISA [32, 33] for GWs, in conjunction with the angular scale of Baryon Acoustic Oscillations (BAO) anticipated by ongoing and forthcoming experiments such as DESI [34, 35] and Euclid [36–38], we argue that it is possible to extrapolate the value of the sound horizon at the baryon drag epoch with a relative uncertainty of  $\sim 1.5\%$ , making no assumption about the cosmological model. Since the sound horizon encapsulates information about the Universe’s expansion history from (soon after) the hot Big Bang singularity all the way up to recombination, this estimate can gauge early-time solutions, potentially confirming or ruling out new physics beyond  $\Lambda$ CDM with a statistical significance approaching 4 standard deviations.

## II. METHODOLOGY

To obtain a model-independent estimate of the sound horizon at the baryon-drag epoch,<sup>5</sup> we propose using the very simple relationship that links  $r_d$  and the angular scale of baryon acoustic oscillations:

$$\theta_{\text{BAO}}(z) = \frac{r_d}{(1+z)D_A(z)} = \frac{(1+z)r_d}{D_L(z)}, \quad (1)$$

where, in the second equality, we have assumed the Distance Duality Relation (DDR),  $D_L(z) = (1+z)^2 D_A(z)$ ,

<sup>5</sup> It’s important to highlight that BAO measurements are sensitive to the sound horizon evaluated at the baryon drag epoch, commonly denoted by  $r_d$  [39]. Conversely, the scale pertinent to the acoustic peaks in the CMB is the sound horizon evaluated at recombination, typically denoted by  $r_s(z_*)$  [40]. These two epochs are separated in redshift by  $\Delta z = z_d - z_* \sim 30$ .

which connects the luminosity distance  $D_L(z)$  to the angular diameter distance  $D_A(z)$  at any redshift  $z$ .<sup>6</sup>

Starting from this relation, we can isolate  $r_d$  and express it in terms of  $\theta_{\text{BAO}}(z)$  and  $D_L(z)$ . In principle, both of these quantities are directly measurable from current and future probes. So the next step involves identifying the most suitable datasets for estimating them.

- Acquiring a dataset capable of providing standard candles for measuring the luminosity distance,  $D_L(z)$ , independently of any calibration methodologies or cosmological model assumptions, requires careful consideration. Although Type-Ia Supernovae serve as "standardizable" candles, they require calibration. Recent discussions have emphasized that the best achievable inference from supernovae data is the quantity  $r_d h$  (where  $H_0 = 100h$  km/s/Mpc) [41], which does not provide sufficient information to address the nature of the Hubble tension and test new physics prior to recombination. Therefore, we suggest leveraging future gravitational wave observations as standard sirens to estimate  $D_L^{\text{GW}}(z_{\text{GW}})$ . Planned experiments such as the Einstein Telescope (ET) and the Laser Interferometer Space Antenna (LISA) are expected to accurately measure the luminosity distance across a wide redshift range  $z_{\text{GW}} \in [z_{\text{GW}}^{\text{min}}, z_{\text{GW}}^{\text{max}}]$  that, depending on the specific experiment, can range from  $z_{\text{GW}}^{\text{min}} \sim 0.1$  up to  $z_{\text{GW}}^{\text{max}} \sim 8$ .<sup>7</sup>
- Measurements of the angular scales of BAOs have been released by several independent groups, extracting  $\theta_{\text{BAO}}(z)$  from diverse catalogues, including those provided by the BOSS and eBOSS surveys [42–44]. However, ongoing and forthcoming large-scale structure experiments, such as Euclid and DESI, are poised to significantly enhance the precision in estimating  $\theta_{\text{BAO}}(z)$  across a redshift window  $z_{\text{BAO}} \in [z_{\text{BAO}}^{\text{min}}, z_{\text{BAO}}^{\text{max}}]$ , spanning from  $z_{\text{BAO}}^{\text{min}} \sim 0.1$  to  $z_{\text{BAO}}^{\text{max}} \sim 2$ , contingent upon the specifics of the experiment.<sup>8</sup> To avoid mixing up current and forecast datasets, we focus on the anticipated improvements brought forth by DESI and Euclid-like experiments on  $\theta_{\text{BAO}}(z)$ , generating mock datasets for both surveys by following the methodology outlined in Appendix A.

Exploring various combinations of mock datasets from future BAO and GW surveys, we aim to forecast the

<sup>6</sup> This relation is quite general and is valid for any cosmological model where spacetime is described by a pseudo-Riemannian manifold, photons propagate along null geodesics, and their number is conserved over time.

<sup>7</sup> ET will reach  $z_{\text{GW}}^{\text{max}} \approx 2.5$ , while LISA will cover redshifts up to  $z_{\text{GW}}^{\text{max}} \approx 8$ , see Appendix B for details.

<sup>8</sup> DESI is covering redshifts  $z_{\text{BAO}}^{\text{min}} \approx 0.15$  to  $z_{\text{BAO}}^{\text{max}} \approx 1.85$ , while Euclid is anticipated to collect data from  $z_{\text{BAO}}^{\text{min}} \approx 0.65$  to  $z_{\text{BAO}}^{\text{max}} \approx 2.05$ .

Redshift	DESI+ET	DESI+LISA	EUCLID+ET	EUCLID+LISA
0.15	4.3%	3.5%	–	–
0.25	7.5%	2.2%	–	–
0.35	9.7%	1.7%	–	–
0.45	11.5%	1.5%	–	–
0.55	13.1%	1.4%	–	–
0.65	14.8%	1.5%	14.2%	1.6%
0.75	16.2%	1.6%	15.5%	1.5%
0.85	17.5%	1.8%	16.9%	1.7%
0.95	18.6%	2.0%	18.2%	1.9%
1.05	19.6%	2.2%	19.5%	2.3%
1.15	20.4%	2.5%	20.6%	2.7%
1.25	21.2%	2.7%	21.5%	3.1%
1.35	21.8%	2.9%	22.2%	3.4%
1.45	22.4%	3.2%	22.6%	3.8%
1.55	22.9%	3.6%	22.8%	4.2%
1.65	23.5%	4.2%	23.0%	4.8%
1.75	24.0%	5.2%	23.2%	5.8%
1.85	24.6%	6.2%	23.3%	5.4%
1.95	–	–	23.5%	6.0%
2.05	–	–	24.12%	7.9%

Table I. Forecasted relative precision  $\sigma_{r_d}/r_d$  on the sound horizon, derived from gravitational wave and baryon acoustic oscillation angular scale measurements by different combinations of surveys including ET and LISA for GWs, and DESI and Euclid for BAO.

precision achievable in determining  $r_d$  independently of any specific cosmological model. One significant challenge underlying the analysis arises from the fact that gravitational wave and BAO measurements will collect data at different redshifts,  $z_{\text{GW}} \neq z_{\text{BAO}}$ . To overcome this difficulty, we propose employing ML regression techniques, specifically ANN. As outlined Appendix B, ANN can be trained to reconstruct the luminosity distance function,  $D_L^{\text{GW}}(z)$ , using gravitational wave observations  $D_L^{\text{GW}}(z_{\text{GW}})$ . Subsequently, these trained ANNs can extrapolate the luminosity distance to the same redshifts as BAO measurements:  $D_L^{\text{GW}}(z_{\text{BAO}})$ .<sup>9</sup> In this way, we can obtain several independent estimates of  $r_d$  – each corresponding to a BAO measurement:

$$r_d = \frac{\theta_{\text{BAO}}(z_{\text{BAO}})D_L^{\text{GW}}(z_{\text{BAO}})}{1 + z_{\text{BAO}}}. \quad (2)$$

Based on the specifications of the various experiments under consideration, we identify a redshift range for each combination of datasets wherein both uncertainties and systematic errors are well under control. Sticking to these redshift ranges, we extract conservative yet informative

estimates regarding the forecast precision of our measurement of the sound horizon,  $\sigma_{r_d}$ . For further technical details on this matter, we refer to Appendix B.

### III. RESULTS

In Tab. I, we summarize the relative precision we forecast on the sound horizon by combining measurements of gravitational waves and baryon acoustic oscillations from various surveys at different redshifts.

At first glance, we note that when dealing with combinations involving ET, the uncertainties are quite substantial. For ET+Euclid, the percentage relative precision  $\sigma_{r_d}/r_d$  consistently exceeds 10%, reaching nearly 20% at  $z \sim 1$ . These significant uncertainties arise from the fact that Euclid will be able to collect BAO measurements primarily at high redshifts  $z \gtrsim 0.6$ , where both the error bars of ET and the scatter of the mock data around the fiducial cosmology notably increase. This leads to broader uncertainty in the ML reconstruction of  $D_L^{\text{GW}}(z)$  and, consequently, in the inferred value of  $r_d$ . On the other hand, combining DESI and ET allows for a significant reduction in uncertainties. This is because DESI is able to gather BAO measurements at lower redshifts where ET will observe more GW events with higher precision, resulting in a more accurate reconstruction of  $D_L^{\text{GW}}(z)$ . However, even with this overall improvement, the most optimistic estimate still yields  $\sigma_{r_d}/r_d \gtrsim 4\%$ , which remains comparable to the changes needed in  $r_d$  to resolve the Hubble tension.<sup>10</sup> Moreover, uncertainties increase rapidly within the redshift range  $z \sim 0.25 - 0.55$ , far exceeding  $\sigma_{r_d}/r_d \gtrsim 10\%$ . Therefore, the primary lesson we can glean is that the combinations of datasets involving ET are not ideal for achieving an informative model-independent measurement of  $r_d$ . Such an estimate would carry uncertainties so significant that it would be practically unusable for assessing new physics at early times.

Looking at the brighter side, a substantial improvement in constraining the value of the sound horizon occurs when we focus on LISA. Despite the fewer number of GW events expected from this survey, the error bars will be significantly reduced compared to ET, leading to a more precise reconstruction of the luminosity distance across the redshifts probed by DESI and Euclid. In this case, the constraining power achieved by combining LISA with either DESI or Euclid is similar: in both cases, we can select a notable redshift window ( $z \lesssim 1$ ) where the uncertainties in the inferred value of the sound horizon remain  $\sigma_{r_d}/r_d \lesssim 2\%$ . In the most optimistic scenario, the uncertainties can be as small as  $\sigma_{r_d}/r_d \lesssim 1.5\%$ .

<sup>9</sup> It is worth noting that GW data points are anticipated to outnumber BAO data points significantly. Therefore, we opt to reconstruct  $D_L^{\text{GW}}(z)$  and estimate it at the same redshift as BAO measurements to enhance ML performance.

<sup>10</sup> We recall that to resolve the Hubble tension, early-time new physics should operate to decrease the value of the sound horizon by approximately  $\Delta r_d/r_d \sim 5 - 6\%$  [14, 25, 45].

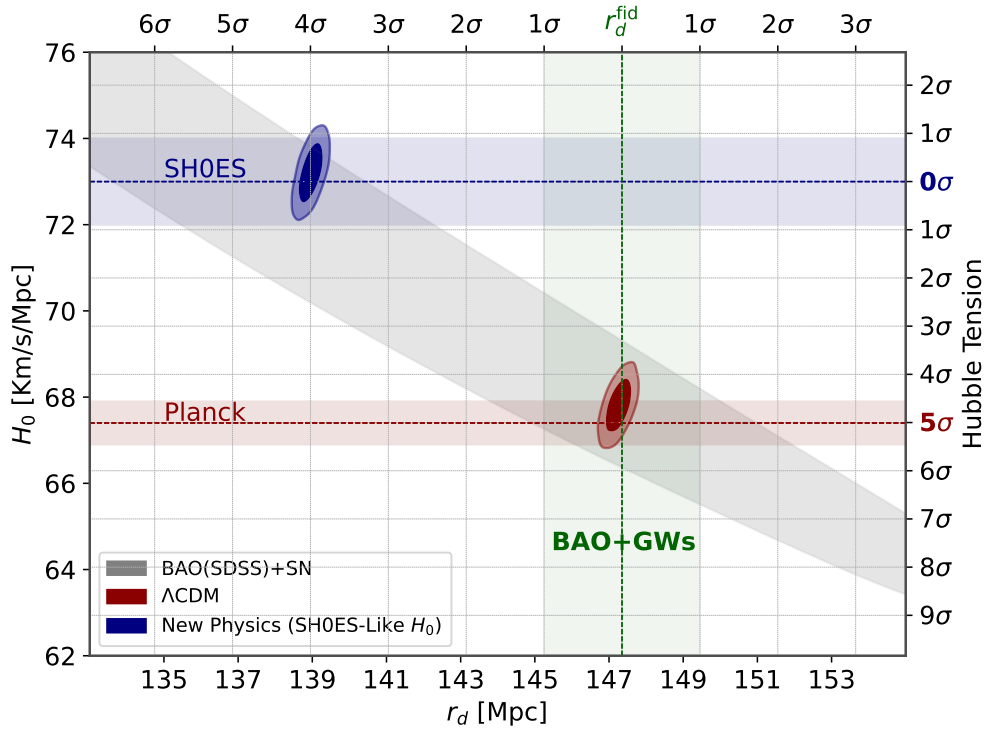


Figure 1. Illustrative plot in the  $r_d - H_0$  plane of the consistency test proposed to assess the possibility of new physics prior to recombination for solving the Hubble constant tension. The red band represents the present value of  $H_0$  measured by the Planck collaboration within a standard  $\Lambda$ CDM model of cosmology, whereas the 2D contours represent the marginalized 68% and 95% CL constraints obtained from the Planck-2018 data. The grey band represents the 95% CL region of the plane identified by analyzing current BAO measurements from the SDSS collaboration and Type Ia supernovae from the Pantheon+ catalogue. The horizontal blue band represents the value of the Hubble constant measured by the SH0ES collaboration. In order to reconcile all the datasets, a potential model of early-time new physics should shift the  $\Lambda$ CDM red contours along the grey band until the grey band overlaps with the SH0ES result. This scenario is depicted by the 2D blue contours obtained under the assumption that the model of new physics does not increase uncertainties on parameters compared to  $\Lambda$ CDM. The green vertical band represents the model-independent value of the sound horizon we are able to extract from combinations of GW data from LISA and BAO measurements (either from DESI-like or Euclid-like experiments) assuming a fiducial  $\Lambda$ CDM baseline cosmology. As is clear from the top x-axis, this value would be able to confirm or rule out the possibility of new physics at about  $4\sigma$ .

To demonstrate that a model-independent estimate of the sound horizon with a precision  $\sigma_{r_d}/r_d \sim 1.5\%$  could decisively clarify the debate on early and late-time solutions while confirming or ruling out new physics beyond the standard cosmological model with high statistical significance, we propose the following conceptual exercise as a proof of concept. First, we suppose that the Hubble tension could indeed indicate the presence of new physics beyond the standard cosmological model. Second, we suppose the existence of an effective realization of early-time new physics – though currently unknown – that can reconcile the discrepancy. While remaining agnostic about the specific solution, we can outline the characteristics it must satisfy:

1. **Maintaining consistency with BAO and SN:** The solution must be consistent with all current cosmological datasets, including measurements of BAO and SN. As discussed in the literature [14], the combination of SN and BAO data defines a band in the  $r_d - H_0$  plane. In Fig. 1, we show in gray the 95% Confidence Level (CL) region of the

parameter space defined by combining the SN gathered from the Pantheon Plus sample with BAO measurements released by the SDSS collaboration. Maintaining consistency with SN and BAO requires moving along this gray band.

2. **Consistency with SH0ES:** The solution must provide an  $H_0$  value in agreement with the current local distance ladder estimate reported by the SH0ES collaboration, represented by the blue horizontal band in Fig. 1. Therefore, as we move along the gray band, we must intersect the blue band. A viable solution should lie at the intersection of the blue and gray bands in Fig. 1, implying a significant reduction in the sound horizon, as has been argued in the literature.
3. **Genuine Solution:** The solution must fit well with CMB data and genuinely resolve the tension by shifting the CMB contours for  $\Lambda$ CDM in the direction indicated by other datasets, ideally maintaining uncertainties in the Bayesian infer-

ence of cosmological parameters comparable to that achieved within the standard  $\Lambda$ CDM scenario.

By imposing these three conditions, we can anticipate where the 2D probability contours that any hypothetical effective solution to the Hubble tension should place in the  $r_d$ - $H_0$  plane. Our ideal scenario is depicted in Fig. 1 with the blue 2D contours for the model that could resolve the Hubble tension. In the figure, we remain somewhat conservative and impose that the blue contours lie as close as possible to those obtained from the standard cosmological model – that is, we consider the *smallest* possible reduction in the value of the sound horizon that can fully satisfy these requirements.<sup>11</sup> Starting from this ideal scenario, we pose the following questions: supposing a theoretical physicist somewhere in the world, perhaps in the (near) future, realizes the solution represented by the blue contours in Fig. 1, (i) is it possible to independently test this solution using the methodology introduced in this article, and (ii) to what level of significance can we confirm or reject the hypothesis of new physics?

To address our questions, we can refer back to Fig. 1, where we illustrate the forecast obtained by assuming a standard  $\Lambda$ CDM cosmological model for the sound horizon, derived from a combination of data involving LISA, with a relative uncertainty of 1.5%. As evident from the figure, a simple independent estimate of the sound horizon would represent a remarkable consistency test for  $\Lambda$ CDM, dismissing the hypothesis of new physics at a statistical significance exceeding 4 standard deviations (refer to the  $x$ -axis at the top of the figure). At this point, only two possibilities would remain on the table: the first would be to assume that the Hubble tension is due to systematics. This possibility, in turn, can be tested with gravitational waves as standard sirens, which will precisely measure  $H_0$  [46, 47], confirming or rejecting the measurement obtained from SH0ES. If the Hubble tension were confirmed, then this would necessarily imply the need to resort to a different physical mechanism than the one proposed by early-time solutions. In our ideal scenario to resolve the problem, we will need to shift the red contours in Fig. 1 vertically and force the cosmological model to lie at the intersection between the green and blue horizontal bands. This possibility would be in strong tension with the gray contours derived from current SN and BAO measurements; thus, it appears less plausible.

On the flip side, it is worth noting that this argument works in reverse, too. If the hypothetical theoretical physicist happens to have stumbled upon the correct solution, our test would yield a model-independent

measurement of the sound horizon consistent with that predicted by the model of new physics, thereby ruling out the value inferred within the standard cosmological framework at 4 standard deviations.

In conclusion, we stress that the significance of the test we proposed lies in the fact that gravitational wave standard sirens will not only be able to assess if the Hubble tension exists in the first place (as extensively discussed in the literature). Should the tension be confirmed, making no assumption on the cosmological model, we will be able to extract model-independent measurements of the sound horizon with a precision competitive with current model-dependent estimates from early Universe probes. This will allow us to test whether the value of the sound horizon is consistent with those predicted by the standard cosmological model, providing an important tool to shed light on the nature of the tension itself. Among other things, this will clarify once and for all the debate on early vs late-time solutions and set clear model-building guidelines for assessing possible new physics beyond  $\Lambda$ CDM.

#### IV. CONCLUSION

In this work, we propose a method for measuring the sound horizon at the baryon drag epoch,  $r_d$ , independently of the cosmological model. Our methodology is based on the relationship linking the angular scale of baryon acoustic oscillations and the angular diameter distance. Assuming that spacetime is described by a pseudo-Riemannian manifold, photons propagate along null geodesics, and their number is conserved over time, we can use the distance duality relation to connect  $\theta_{\text{BAO}}(z)$  and  $D_L(z)$  by means of Eq. (1). Starting from this relation, we propose using future gravitational waves as standard sirens to gather precise measurements of the luminosity distance in the Universe, which are free from calibration methods compared to current "standardizable" candles such as Type-Ia supernovae.

We argue that employing machine learning techniques, particularly artificial neural network linear regression, one can combine future gravitational wave observations from LISA with angular BAO measurements, either from DESI-like or Euclid-like surveys, enabling us to obtain model-independent estimates of the sound horizon. In the redshift range  $z \lesssim 1$ , we forecast that the relative precision of these estimates will be as small as  $\sigma_{r_d}/r_d \sim 1.5\%$ . This would offer a *unique* model-independent measure of a fundamental scale characterizing the early universe, with a precision competitive to values inferred within specific theoretical frameworks, including the standard cosmological model. Such measurements have several significant implications:

- (i) **Providing a consistency test for the standard cosmological model:** We can test the value of  $r_d$  predicted by the baseline cosmological model with high statistical significance, either confirming its

<sup>11</sup> Note that we could horizontally shift the 2D blue contours towards the left of the  $x$ -axis in Fig. 1 while maintaining good agreement with all the three requirements we impose. This situation will imply a larger reduction in the sound horizon, increasing our ability to detect the change. In this sense, we work under reasonably conservative conditions.

predictions or providing hints of new physics beyond  $\Lambda$ CDM.

- (ii) **Shedding light on the nature of the Hubble tension:** If the tension is confirmed by gravitational wave standard sirens, our test could provide crucial information about its nature. In particular, we will be able to conclusively assess if the Hubble tension requires new physics acting prior to recombination to reduce the value of the sound horizon. As shown in this work, we can draw some general model-agnostic guidelines from current data that give solid grounds to believe that a compelling early-time solution would require a reduction of about 5-6% in the value of the sound horizon. Such a hypothesis can be confirmed or ruled out at least at  $4\sigma$  by our test, see also Fig. 1.
- (iii) **Providing a definitive answer about the debate surrounding early vs late-time solutions of the Hubble tension:** Should the Hubble tension be confirmed by gravitational wave standard sirens, leading to a necessary paradigm shift in cosmological modeling, our test can provide definitive guidelines. It will decisively address the ongoing

debate between early and late-time solutions. On one hand, the detection of new physics from the early universe with high statistical significance could bolster early-time solutions, challenging the late-time community. Conversely, if our test confirms the sound horizon value predicted by the  $\Lambda$ CDM model, it would undermine early-time solutions, thus favoring alternative late-time proposals.

## ACKNOWLEDGMENTS

We thank Elsa M. Teixeira and Richard Daniel for the help and useful discussions. WG and CvdB are supported by the Lancaster–Sheffield Consortium for Fundamental Physics under STFC grant: ST/X000621/1. EDV is supported by a Royal Society Dorothy Hodgkin Research Fellowship. This article is based upon work from COST Action CA21136 Addressing observational tensions in cosmology with systematics and fundamental physics (CosmoVerse) supported by COST (European Cooperation in Science and Technology). We acknowledge IT Services at The University of Sheffield for the provision of services for High Performance Computing.

- 
- [1] A. G. Riess et al., *Astrophys. J. Lett.* **934**, L7 (2022), [arXiv:2112.04510 \[astro-ph.CO\]](#).
- [2] Y. S. Murakami, A. G. Riess, B. E. Stahl, W. D. Kenworthy, D.-M. A. Pluck, A. Macoreta, D. Brout, D. O. Jones, D. M. Scolnic, and A. V. Filippenko, *JCAP* **11**, 046 (2023), [arXiv:2306.00070 \[astro-ph.CO\]](#).
- [3] L. Breuval, A. G. Riess, S. Casertano, W. Yuan, L. M. Macri, M. Romaniello, Y. S. Murakami, D. Scolnic, G. S. Anand, and I. Soszyński, (2024), [arXiv:2404.08038 \[astro-ph.CO\]](#).
- [4] N. Aghanim et al. (Planck), *Astron. Astrophys.* **641**, A6 (2020), [Erratum: *Astron. Astrophys.* 652, C4 (2021)], [arXiv:1807.06209 \[astro-ph.CO\]](#).
- [5] A. G. Riess, G. S. Anand, W. Yuan, S. Casertano, A. Dolphin, L. M. Macri, L. Breuval, D. Scolnic, M. Perrin, and I. R. Anderson, *Astrophys. J. Lett.* **962**, L17 (2024), [arXiv:2401.04773 \[astro-ph.CO\]](#).
- [6] D. Brout and A. Riess, (2023), [arXiv:2311.08253 \[astro-ph.CO\]](#).
- [7] P. Agrawal, F.-Y. Cyr-Racine, D. Pinner, and L. Randall, *Phys. Dark Univ.* **42**, 101347 (2023), [arXiv:1904.01016 \[astro-ph.CO\]](#).
- [8] E. Di Valentino, O. Mena, S. Pan, L. Visinelli, W. Yang, A. Melchiorri, D. F. Mota, A. G. Riess, and J. Silk, *Class. Quant. Grav.* **38**, 153001 (2021), [arXiv:2103.01183 \[astro-ph.CO\]](#).
- [9] N. Schöneberg, G. Franco Abellán, A. Pérez Sánchez, S. J. Witte, V. Poulin, and J. Lesgourgues, *Phys. Rept.* **984**, 1 (2022), [arXiv:2107.10291 \[astro-ph.CO\]](#).
- [10] E. Abdalla et al., *JHEAp* **34**, 49 (2022), [arXiv:2203.06142 \[astro-ph.CO\]](#).
- [11] V. Poulin, T. L. Smith, and T. Karwal, *Phys. Dark Univ.* **42**, 101348 (2023), [arXiv:2302.09032 \[astro-ph.CO\]](#).
- [12] A. R. Khalife, M. B. Zanjani, S. Galli, S. Günther, J. Lesgourgues, and K. Benabed, *JCAP* **04**, 059 (2024), [arXiv:2312.09814 \[astro-ph.CO\]](#).
- [13] W. Giarè, (2024), [arXiv:2404.12779 \[astro-ph.CO\]](#).
- [14] L. Knox and M. Millea, *Phys. Rev. D* **101**, 043533 (2020), [arXiv:1908.03663 \[astro-ph.CO\]](#).
- [15] K. Jedamzik, L. Pogosian, and G.-B. Zhao, *Commun. in Phys.* **4**, 123 (2021), [arXiv:2010.04158 \[astro-ph.CO\]](#).
- [16] S. Vagnozzi, *Universe* **9**, 393 (2023), [arXiv:2308.16628 \[astro-ph.CO\]](#).
- [17] E. Di Valentino, *Universe* **8**, 399 (2022).
- [18] G. Efstathiou, *Mon. Not. Roy. Astron. Soc.* **505**, 3866 (2021), [arXiv:2103.08723 \[astro-ph.CO\]](#).
- [19] C. Krishnan, R. Mohayaee, E. O. Colgáin, M. M. Sheikh-Jabbari, and L. Yin, *Class. Quant. Grav.* **38**, 184001 (2021), [arXiv:2105.09790 \[astro-ph.CO\]](#).
- [20] R. E. Keeley and A. Shafieloo, *Phys. Rev. Lett.* **131**, 111002 (2023), [arXiv:2206.08440 \[astro-ph.CO\]](#).
- [21] S. Gariazzo, W. Giarè, O. Mena, and E. Di Valentino, (2024), [arXiv:2404.11182 \[astro-ph.CO\]](#).
- [22] A. G. Adame et al. (DESI), (2024), [arXiv:2404.03000 \[astro-ph.CO\]](#).
- [23] A. G. Adame et al. (DESI), (2024), [arXiv:2404.03001 \[astro-ph.CO\]](#).
- [24] D. Collaboration, “Desi 2024 vi: Cosmological constraints from the measurements of baryon acoustic oscillations,” (2024), [arXiv:2404.03002 \[astro-ph.CO\]](#).
- [25] W. Giarè, M. A. Sabogal, R. C. Nunes, and E. Di Valentino, (2024), [arXiv:2404.15232 \[astro-ph.CO\]](#).
- [26] D. Wang, (2024), [arXiv:2404.06796 \[astro-ph.CO\]](#).
- [27] M. Cortès and A. R. Liddle, (2024), [arXiv:2404.08056 \[astro-ph.CO\]](#).
- [28] E. O. Colgáin, M. G. Dainotti, S. Capozziello, S. Pouro-

- jaghi, M. M. Sheikh-Jabbari, and D. Stojkovic, (2024), [arXiv:2404.08633 \[astro-ph.CO\]](#).
- [29] W. Yin, (2024), [arXiv:2404.06444 \[hep-ph\]](#).
- [30] O. Seto and Y. Toda, (2024), [arXiv:2405.11869 \[astro-ph.CO\]](#).
- [31] B. R. Dinda, (2024), [arXiv:2405.06618 \[astro-ph.CO\]](#).
- [32] E. Belgacem et al. (LISA Cosmology Working Group), *JCAP* **07**, 024 (2019), [arXiv:1906.01593 \[astro-ph.CO\]](#).
- [33] P. Auclair et al. (LISA Cosmology Working Group), *Living Rev. Rel.* **26**, 5 (2023), [arXiv:2204.05434 \[astro-ph.CO\]](#).
- [34] M. Levi et al. (DESI), (2013), [arXiv:1308.0847 \[astro-ph.CO\]](#).
- [35] A. Aghamousa et al. (DESI), (2016), [arXiv:1611.00036 \[astro-ph.IM\]](#).
- [36] R. Laureijs et al. (EUCLID), (2011), [arXiv:1110.3193 \[astro-ph.CO\]](#).
- [37] L. Amendola et al. (Euclid Theory Working Group), *Living Rev. Rel.* **16**, 6 (2013), [arXiv:1206.1225 \[astro-ph.CO\]](#).
- [38] L. Amendola et al., *Living Rev. Rel.* **21**, 2 (2018), [arXiv:1606.00180 \[astro-ph.CO\]](#).
- [39] E. Aubourg et al. (BOSS), *Phys. Rev. D* **92**, 123516 (2015), [arXiv:1411.1074 \[astro-ph.CO\]](#).
- [40] W. Hu and S. Dodelson, *Ann. Rev. Astron. Astrophys.* **40**, 171 (2002), [arXiv:astro-ph/0110414](#).
- [41] T. Liu, X. Zhong, J. Wang, and M. Biesiada, (2024), [arXiv:2405.12498 \[astro-ph.CO\]](#).
- [42] R. C. Nunes, S. K. Yadav, J. F. Jesus, and A. Bernui, *Mon. Not. Roy. Astron. Soc.* **497**, 2133 (2020), [arXiv:2002.09293 \[astro-ph.CO\]](#).
- [43] E. de Carvalho, A. Bernui, F. Avila, C. P. Novaes, and J. P. Nogueira-Cavalcante, *Astron. Astrophys.* **649**, A20 (2021), [arXiv:2103.14121 \[astro-ph.CO\]](#).
- [44] R. Menote and V. Marra, *Mon. Not. Roy. Astron. Soc.* **513**, 1600 (2022), [arXiv:2112.10000 \[astro-ph.CO\]](#).
- [45] S. Vagnozzi, *Phys. Rev. D* **102**, 023518 (2020), [arXiv:1907.07569 \[astro-ph.CO\]](#).
- [46] H.-Y. Chen, M. Fishbach, and D. E. Holz, *Nature* **562**, 545 (2018), [arXiv:1712.06531 \[astro-ph.CO\]](#).
- [47] A. Palmese et al., (2019), [arXiv:1903.04730 \[astro-ph.CO\]](#).
- [48] N. Aghanim et al. (Planck), *Astron. Astrophys.* **641**, A6 (2020), [Erratum: *Astron. Astrophys.* 652, C4 (2021)], [arXiv:1807.06209 \[astro-ph.CO\]](#).
- [49] J. Lesgourgues, “The cosmic linear anisotropy solving system (class) i: Overview,” (2011), [arXiv:1104.2932 \[astro-ph.IM\]](#).
- [50] D. Blas, J. Lesgourgues, and T. Tram, *Journal of Cosmology and Astroparticle Physics* **2011**, 034–034 (2011).
- [51] J. Lesgourgues, “The cosmic linear anisotropy solving system (class) iii: Comparison with camb for  $\Lambda$ -CDM,” (2011), [arXiv:1104.2934 \[astro-ph.CO\]](#).
- [52] E. Di Valentino, D. E. Holz, A. Melchiorri, and F. Renzi, *Phys. Rev. D* **98**, 083523 (2018), [arXiv:1806.07463 \[astro-ph.CO\]](#).
- [53] W. Giarè, F. Renzi, A. Melchiorri, O. Mena, and E. Di Valentino, *Mon. Not. Roy. Astron. Soc.* **511**, 1373 (2022), [arXiv:2110.00340 \[astro-ph.CO\]](#).
- [54] A. Font-Ribera, P. McDonald, N. Mostek, B. Reid, H.-J. Seo, and A. Slosar, *Journal of Cosmology and Astroparticle Physics* **2014** (2014), 10.1088/1475-7516/2014/05/023.
- [55] L. A. Escamilla, W. Giarè, E. D. Valentino, R. C. Nunes, and S. Vagnozzi, **2024**, 091 (2024).
- [56] E. M. Teixeira, R. Daniel, N. Frusciante, and C. van de Bruck, *Phys. Rev. D* **108**, 084070 (2023), [arXiv:2309.06544 \[astro-ph.CO\]](#).
- [57] A. Nishizawa, A. Taruya, and S. Saito, *Phys. Rev. D* **83**, 084045 (2011).
- [58] C. Caprini and N. Tamanini, *Journal of Cosmology and Astroparticle Physics* **2016**, 006 (2016).
- [59] G.-J. Wang, X.-J. Ma, S.-Y. Li, and J.-Q. Xia, *Astrophys. J. Suppl.* **246**, 13 (2020), [arXiv:1910.03636 \[astro-ph.CO\]](#).
- [60] J. Lee, Y. Bahri, R. Novak, S. S. Schoenholz, J. Pennington, and J. Sohl-Dickstein, (2017), [arXiv:1711.00165 \[stat.ML\]](#).
- [61] D.-A. Clevert, T. Unterthiner, and S. Hochreiter, *arXiv e-prints* (2016), [arXiv:1511.07289](#).
- [62] Y. A. LeCun, L. Bottou, G. B. Orr, and K.-R. Müller, “Efficient backprop,” in *Neural Networks: Tricks of the Trade: Second Edition*, edited by G. Montavon, G. B. Orr, and K.-R. Müller (Springer Berlin Heidelberg, Berlin, Heidelberg, 2012) pp. 9–48.
- [63] D. P. Kingma and J. Ba, (2017), [arXiv:1412.6980 \[cs.LG\]](#).
- [64] J. Torrado and A. Lewis, *Journal of Cosmology and Astroparticle Physics* **2021**, 057 (2021).

## Appendix A: Forecasts of the BAO Angular Scale

To generate forecasted measurements, both for the angular BAO and gravitational waves (detailed in the next appendix), we adopt a fiducial  $\Lambda$ CDM cosmological model. We set the values of cosmological parameters to their best-fit values from the Planck 2018 analysis [48], as summarized in Table II. Fixing these parameter values, we derive other relevant quantities and compute the theoretical model using the Boltzmann solver code CLASS [49–51].

To forecast the angular BAO scale,  $\theta_{\text{BAO}}(z)$ , we follow established methods previously employed to test and constrain extensions of  $\Lambda$ CDM [52, 53]. Our focus in this study is on forecasting for the upcoming Dark Energy Spectroscopic Instrument (DESI) [34, 35] and Euclid [36–38] redshift surveys. Starting with the fiducial  $\Lambda$ CDM cosmology, we simulate measurements of the angular diameter distance at the redshifts where DESI-like and Euclid-like experiments are expected to collect data. We assume a realistic relative precision,  $\sigma_{D_A}(z)/D_A(z)$ , which varies with redshift and survey. Information on the redshifts and relative precision is obtained from Table V and Table VI of Ref. [54] for DESI-like and Euclid-like surveys, respectively.

We introduce Gaussian noise in the mock measurements of  $D_A(z)$  to simulate the final observations. Various statistical metrics are considered to determine the appropriate level of scatter around the fiducial value. Ultimately, we adopt the following criterion: for each BAO measurement, we ensure that the difference between the fiducial value and the forecast data point, normalized by the observational uncertainties, is smaller than 1:

$$\frac{|D_A(z) - D_A^{\text{fid}}(z)|}{\sigma_{D_A}(z)} \lesssim 1. \quad (\text{A1})$$

This is already mostly true for current SDSS BAO measurements (see the bottom panel in Fig. 6 of Ref. [55]) and the first data release of DESI (see the bottom panel in Fig. 2 of Ref. [25]).<sup>12</sup>

The BAO angular scale  $\theta_{\text{BAO}}(z)$ , and the corresponding error  $\sigma_\theta(z)$  can then be computed from  $D_A(z)$  and  $\sigma_{D_A}$  as

$$\theta_{\text{BAO}}(z) = \frac{\kappa r_d^{\text{fid}}}{(1+z)D_A(z)}, \quad \sigma_\theta(z) = \frac{\kappa r_d^{\text{fid}} \sigma_{D_A}}{(1+z)D_A(z)^2} \quad (\text{A2})$$

with  $\kappa = 180/\pi$  and  $r_d^{\text{fid}}$  being the sound horizon corresponding to the fiducial  $\Lambda$ CDM cosmology ( $r_d^{\text{fid}} \sim 147$  Mpc). We show in Fig. 2 the forecasted values for  $\theta_{\text{BAO}}(z)$  obtained following this methodology.

<sup>12</sup> We test that this choice does not significantly affect the conclusions reached in this paper, as well as that we can recover the fiducial cosmological model when performing Markov Chain Monte Carlo (MCMC) analyses for these data, see Sec. C.

Parameter	Fiducial Value
$\Omega_b h^2$	0.022383
$\Omega_c h^2$	0.12011
$\log(10^{10} A_s)$	3.0448
$n_s$	0.96605
$100 \theta_{\text{MC}}$	1.040909
$\tau$	0.0543
$\sum m_\nu$ [eV]	0.06

Table II. Fiducial Value of Cosmological Parameters.

## Appendix B: Forecasts of Gravitational Waves as Standard Sirens

To reconstruct the redshift-luminosity distance relation  $D_L(z)$  from gravitational waves used as standard sirens through an artificial neural network, it is essential to have training data consisting of a series of  $D_L(z)$  measurements along with their associated errors  $\sigma_{D_L}$ . In this work, we generate mock data to simulate gravitational wave measurements that are expected from future experiments such as the Einstein Telescope (ET) and the Laser Interferometer Space Antenna (LISA). For producing these data, we strictly follow the methodology proposed in Ref. [56], which we summarize step-by-step below.

### 1. Merger Event Distribution

Given the  $\Lambda$ CDM background cosmology, a redshift distribution of gravitational-wave-generating merger events is generated for each of the ET and LISA experiments based on the events those experiments are designed to detect. For ET, these events are the mergers of binary neutron stars (BNS) and black hole neutron star binaries (BHNS), and follow the distribution  $P$  defined as

$$P \propto \frac{4\pi d_c(z) R(z)}{(1+z)H(z)}, \quad (\text{B1})$$

where  $d_c(z)$  and  $H(z)$  represent the comoving distance and Hubble parameter, respectively. These quantities, for our model of cosmology, are obtained via CLASS at various redshifts.  $R(z)$  is known as the merger rate for BNS and BHNS systems, defined to a linear approximation in Ref. [57] as

$$R(z) = \begin{cases} 1 + 2z & \text{for } z < 1, \\ \frac{3}{4}(5 - z) & \text{for } 1 \leq z < 5, \\ 0 & \text{otherwise.} \end{cases} \quad (\text{B2})$$

In this work, we consider simulated ET events in the range  $0 \leq z \leq 2.5$ . The LISA experiment targets lower

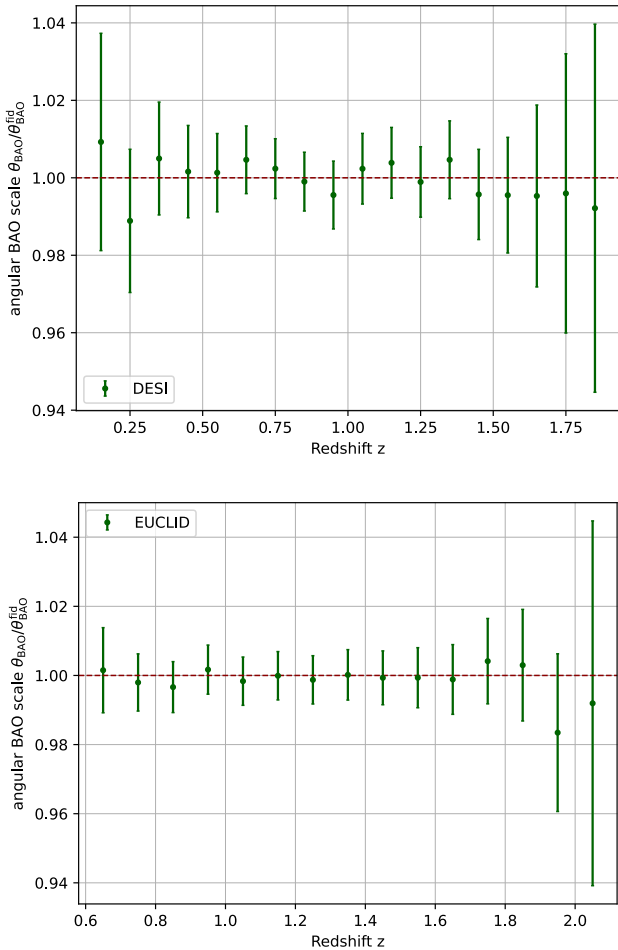


Figure 2. Example forecast for DESI (top panel) and Euclid (bottom panel) observations. The plots show the forecasted values of the BAO angular scale  $\theta_{\text{BAO}}(z)/\theta_{\text{BAO}}^{\text{fid}}(z)$ , where  $\theta_{\text{BAO}}^{\text{fid}}(z)$  is the angular BAO scale predicted by the fiducial  $\Lambda$ CDM cosmology. The error bars indicate the uncertainties in these forecasted values. The forecasted data points are generated based on the expected performance of the DESI and Euclid surveys.

frequencies than ET and therefore focuses on higher-mass binary massive black hole (BMBH) mergers in the range  $0 \leq z \leq 8$ . These events were generated based on the L6A2M5N2 mission distribution [58].

## 2. Simulating $D_L(z)$ Measurements and $\sigma_{D_L}$ Errors

Once the standard siren catalogues  $D_L(z)$  have been generated from their respective redshift distributions, the events that could plausibly be measured by the LISA and ET experiments must be identified, and the error associated with those measurements  $\sigma_{D_L}$  computed. This is done based on the signal-to-noise ratio (SNR) for a given

event. SNR is defined as

$$\text{SNR} = 4 \int_{f_{\text{min}}}^{f_{\text{max}}} \frac{|\mathcal{H}|}{S_h} df, \quad (\text{B3})$$

where  $\mathcal{H}$  is the Fourier transform of the strain on the LISA/ET interferometer and  $S_h$  is the noise power spectral density.  $S_h$  weights the SNR depending on the specific properties of the instruments used in the ET and LISA detectors (see equations 15 and 16 of Ref. [56]). Siren signals in the GW catalogue are discarded as unlikely to be detected by either LISA or ET if  $\text{SNR} < 8$ .

After SNR slicing of the siren catalogue, the error  $\sigma_{D_L}$  is computed using the sum of error contributions

$$\sigma_{D_L} = \sqrt{(\sigma_{D_L}^{\text{inst}})^2 + (\sigma_{D_L}^{\text{len}})^2 + (\sigma_{D_L}^{\text{pec}})^2}, \quad (\text{B4})$$

where  $\sigma_{D_L}^{\text{inst}} \approx 2D_L/\rho$  is the instrumental error in the luminosity distance measurement,  $\sigma_{D_L}^{\text{len}}$  is the error due to gravitational lensing

$$\sigma_{D_L}^{\text{len}} = \frac{D_L}{2} \times 0.066 \left[ 4(1 - (1+z)^{1/4}) \right]^{1.8} \quad (\text{B5})$$

and  $\sigma_{D_L}^{\text{pec}}$  is a factor unique to the orbital LISA experiment ( $\sigma_{D_L}^{\text{pec}} = 0$  for ET) derived from the peculiar velocities of GW sources relative to the Hubble flow

$$\sigma_{D_L}^{\text{pec}} = D_L \frac{\sqrt{\langle v^2 \rangle}}{c} \left[ 1 + \frac{c(1+z)}{HD_L} \right], \quad (\text{B6})$$

with estimate  $\sqrt{\langle v^2 \rangle} = 500 \text{ km s}^{-1}$ .

## 3. ANN Reconstruction of $D_L(z)$

In order to combine  $D_L(z)$  from GW sirens with BAO observations at arbitrary redshifts to compute  $r_d$ , a continuous  $D_L(z)$  function must be reconstructed from the  $D_L(z)$  and  $\sigma_{D_L}$  datasets. This work uses the `refann`<sup>13</sup> code [59] to construct an artificial neural network (ANN)<sup>14</sup> that describes a continuous  $D_L(z)$  function for both the LISA and ET experiments.

Fig. 3 shows the architecture of the ANN used in this work. In general, ANNs consist of an input layer, one or more hidden layers and an output layer. Each layer accepts a vector from the previous layer and applies a weighted linear transformation followed by a nonlinear activation function, before passing the result onto the next layer. It is these weights at each layer of the network that are optimised during supervised training based on

<sup>13</sup> <https://github.com/Guo-Jian-Wang/refann>

<sup>14</sup> ANNs are known to be equivalent to Gaussian Processes in certain limits [60] and are designed for reconstructing functions from precisely this type of data.

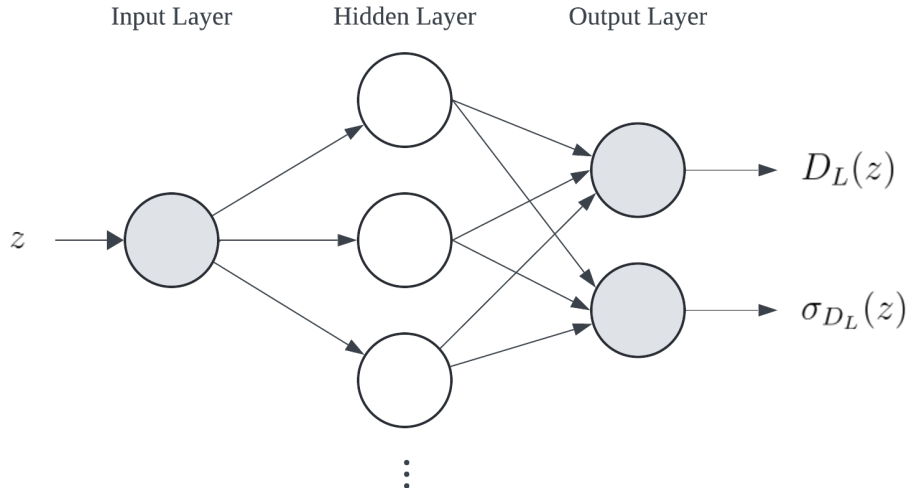


Figure 3. Architecture of the single-hidden-layer ANN used to reconstruct  $D_L$  and  $\sigma_{D_L}$  at input redshift  $z$ .

a chosen loss function against a labelled target output. This process is formalized in vector notation as

$$\mathbf{z}_{i+1} = \mathbf{x}_i \mathbf{W}_{i+1} + \mathbf{b}_{i+1}, \quad (\text{B7})$$

$$\mathbf{x}_{i+1} = f(\mathbf{z}_{i+1}), \quad (\text{B8})$$

where  $\mathbf{x}_i$  is the  $i$ -th layer input vector,  $f$  is the nonlinear activation function and  $\mathbf{W}_{i+1}$  and  $\mathbf{b}_{i+1}$  are the linear weights and biases to be optimised. The ANN in this work uses one hidden layer with an elementwise Exponential Linear Unit [61] activation function

$$f(x) = \begin{cases} x & \text{for } x > 0 \\ e^x - 1 & \text{for } x \leq 0. \end{cases} \quad (\text{B9})$$

In the practical implementation of such a network, these vector processes are performed in batches of inputs  $X \in \mathbb{R}^{l \times n}$  where  $n$  is the dimensionality of each input and  $l$  is the number of inputs in the batch. Equations (B7) and (B8) then become the matrix process

$$Z_{i+1} = X_i W_{i+1} + B_{i+1}, \quad (\text{B10})$$

$$X_{i+1} = f(Z_{i+1}), \quad (\text{B11})$$

such that the ANN can now be understood in terms of the function  $f_{W,B}$  on input  $X$ . In a supervised learning setting, each input in  $X$  is labelled with its corresponding ground-truth output  $Y_{\text{truth}} \in \mathbb{R}^{l \times p}$  where  $p$  is the dimensionality of the output. Training the model then becomes minimizing the difference between predicted outputs  $Y_{n,\text{pred}} = f_{W,B}(X_n)$  and  $Y_{n,\text{truth}}$  for the  $n$ -th input

in  $X$ , by optimizing the parameter sets  $W$  and  $B$ . This is done using the mean-absolute-error function

$$\mathcal{L} = \frac{1}{lp} \|Y_{\text{pred}} - Y_{\text{truth}}\|, \quad (\text{B12})$$

root-mean-squared error was also tested, and a negligible difference in model performance was found. Equation (B12) is then used for optimization of weights  $W$  and biases  $B$  by iterative algorithmic back-propagation. Back-propagation involves computing the following derivatives of  $\mathcal{L}$  [62]:

$$\frac{\partial \mathcal{L}}{\partial Z_{i+1}} = f'(Z_{i+1}) \frac{\partial \mathcal{L}}{\partial X_{i+1}}, \quad (\text{B13})$$

$$\frac{\partial \mathcal{L}}{\partial W_{i+1}} = X_i^T \frac{\partial \mathcal{L}}{\partial Z_{i+1}}, \quad (\text{B14})$$

$$\frac{\partial \mathcal{L}}{\partial X_i} = W_{i+1}^T \frac{\partial \mathcal{L}}{\partial Z_{i+1}}, \quad (\text{B15})$$

$$\frac{\partial \mathcal{L}}{\partial B_{i+1}} = f'(Z_{i+1}) \frac{\partial \mathcal{L}}{\partial X_{i+1}}, \quad (\text{B16})$$

Equations B13-B16 allow the manipulation of the  $i$ -th layer gradients of the ANN from layer  $i+1$ , according to a choice of gradient-descent optimizer. This means that the weights  $W_k$  and biases  $B_k$  of the  $k$ -th training iteration are then updated to new values  $W_{k+1}$  and  $B_{k+1}$  for iteration  $k+1$  such that they descend the gradient of  $\mathcal{L}$ . `refann` uses the Adam optimizer [63], and in this work, we find 30,000 training iterations are sufficient to

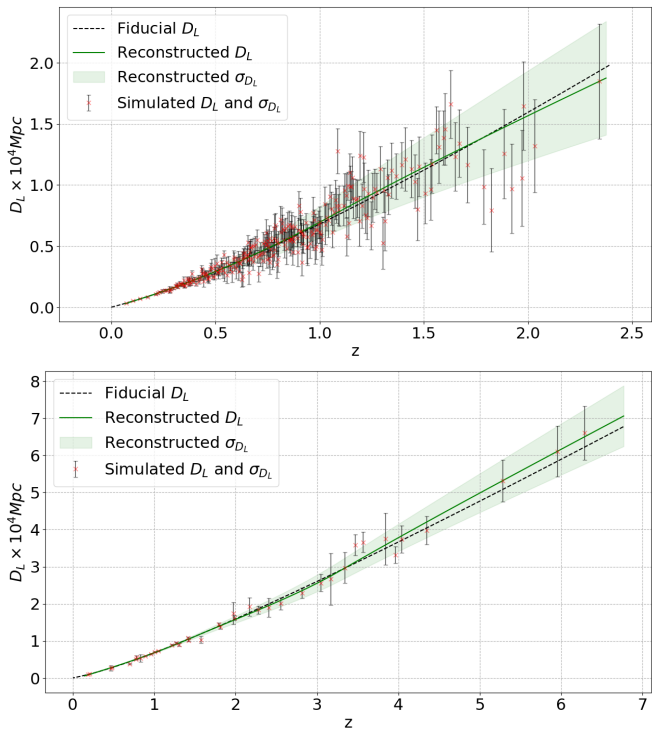


Figure 4. Reconstruction of  $D_L(z)$  and  $\sigma_{D_L}(z)$  from simulated ET gravitational wave sirens in the range  $0 \leq z \leq 2.5$  (top panel) and from simulated LISA gravitational wave sirens in the range  $0 \leq z \leq 8$  (bottom panel).

minimize  $\mathcal{L}$  over a given set of either LISA or ET  $D_L$  and  $\sigma_{D_L}$  data.

Fig. 4 shows the functions  $D_L^{\text{ANN}}(z)$  and associated errors  $\sigma_{D_L}^{\text{ANN}}(z)$  given by models trained on ET and LISA data, respectively. Overall, ET is expected to observe a larger number of GW events from which we can extract a greater number of  $D_L(z)$  measurements compared to LISA. However, it is worth noting that on average, ET has higher uncertainties  $\sigma_{D_L}(z)$  at lower redshifts. In contrast, LISA provides more accurate  $D_L(z)$  measurements across a larger redshift range. Regarding the reconstruction, the ET model fits the majority of the data, although some extraneous data points evade capture. Conversely, the LISA model captures the simulated observational data well but displays significantly higher uncertainties at  $z > 6$  due to the sparsity of events in this redshift range.

#### 4. $r_d$ from $D_L^{\text{ANN}}(z)$ and $\theta_{\text{BAO}}(z)$

Using the ANN model trained on either LISA or ET data, we can reconstruct a continuous function,  $D_L^{\text{ANN}}(z)$ , that can be evaluated at the forecasted  $\theta_{\text{BAO}}(z)$  redshift values. Therefore, Eq. (1) can be used to combine these data into a model-independent estimate of the sound horizon at the baryon-drag epoch,  $r_d$ , and

its uncertainty,  $\sigma_{r_d}$ :

$$r_d = \frac{\theta_{\text{BAO}}(z) D_L^{\text{ANN}}(z)}{(1+z)}, \quad (\text{B17})$$

$$\sigma_{r_d} = \frac{\sqrt{(D_L^{\text{ANN}}(z) \sigma_{\theta_{\text{BAO}}})^2 + (\theta_{\text{BAO}}(z) \sigma_{D_L^{\text{ANN}}})^2}}{(1+z)} \quad (\text{B18})$$

Using forecasts from gravitational wave experiments (ET and LISA) along with forecasts for the angular scale of baryon acoustic oscillations (DESI and Euclid), we have four different pairs of datasets:

- $D_L^{\text{ANN}}(z)$  from ET data and  $\theta_{\text{BAO}}(z)$  from DESI data.
- $D_L^{\text{ANN}}(z)$  from ET data and  $\theta_{\text{BAO}}(z)$  from Euclid data.
- $D_L^{\text{ANN}}(z)$  from LISA data and  $\theta_{\text{BAO}}(z)$  from DESI data.
- $D_L^{\text{ANN}}(z)$  from LISA data and  $\theta_{\text{BAO}}(z)$  from Euclid data.

For any of these four combinations of data, we can obtain several independent estimates of  $r_d$ , along with its corresponding uncertainty. Specifically, we can obtain an estimate for each BAO data point. In Tab. I, we provide the relative precision  $\sigma_{r_d}/r_d$  that we can achieve at different redshifts  $z$ . Instead, in Fig. 5, we show realistic estimates of  $r_d/r_d^{\text{fid}}$  for the four different pairs of datasets described above.

### Appendix C: Consistency Tests

Our method of forecasting the angular BAO scale and the redshift-luminosity distance relation  $D_L(z)$  from gravitational wave events does introduce some artificial randomness in the Gaussian noise used to simulate realistic mock data. As explained in the manuscript, we considered different statistical metrics to introduce a controlled –yet realistic– scatter of data points around the fiducial  $\Lambda$ CDM cosmology. In this appendix, we explicitly test whether the random noise introduced is indeed under control by performing an MCMC test with forecasted data, aimed at checking whether we can recover the fiducial cosmology afterward.

In particular, the simulated BAO and GW data are compared to the theoretical  $\theta(z)$  and  $D_L(z)$  values through a multivariate Gaussian likelihood:

$$-2 \ln \mathcal{L} = \sum (\mu - \hat{\mu}) C^{-1} (\mu - \hat{\mu})^T, \quad (\text{C1})$$

where  $\mu$  and  $\hat{\mu}$  are the vectors containing the simulated and theoretical values  $\theta(z)$  and  $D_L(z)$  at each redshift, and  $C$  is their simulated covariance matrix.<sup>15</sup>

<sup>15</sup> In our mock data, we adopt a diagonal covariance matrix.

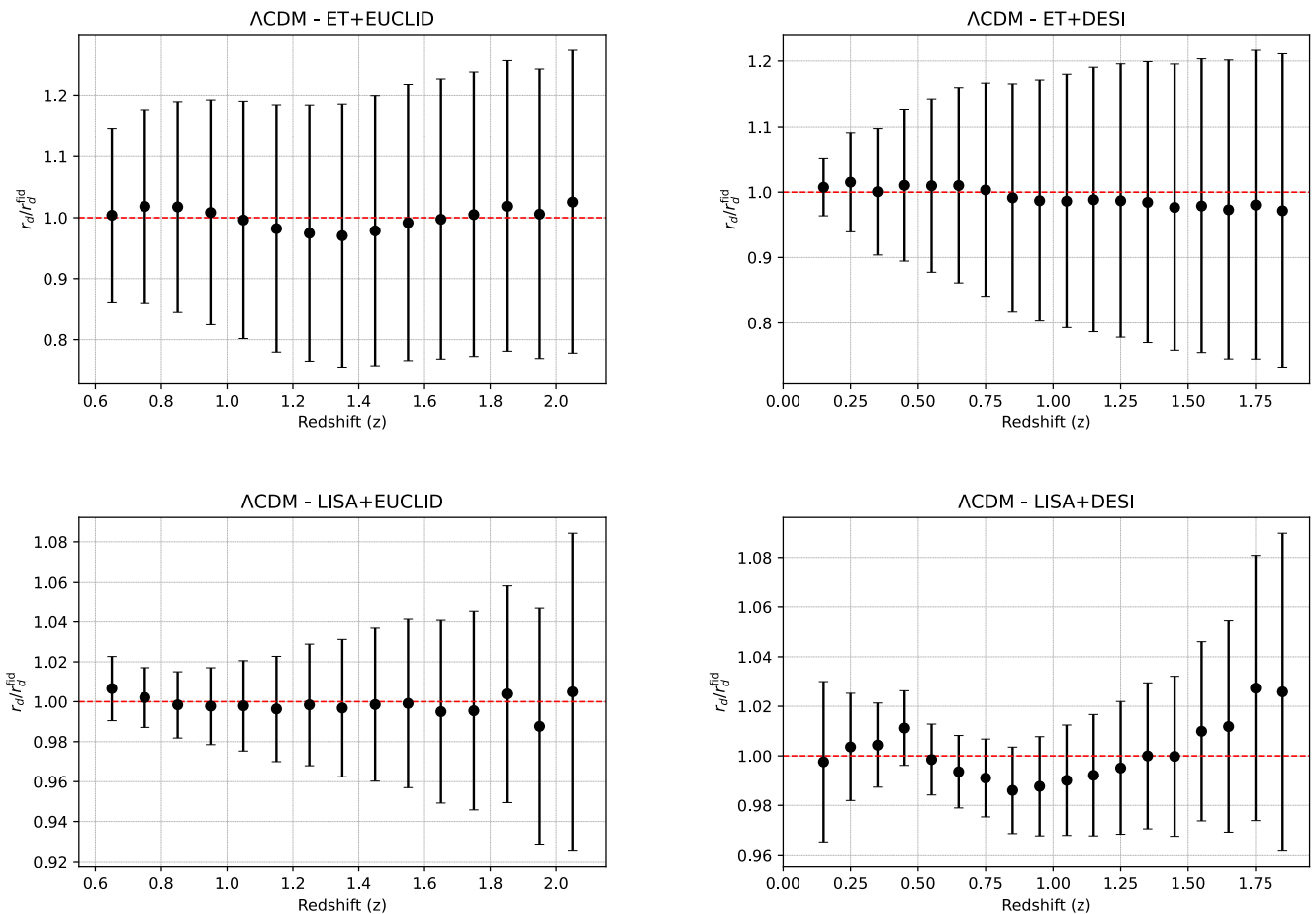


Figure 5. Estimates of  $r_d/r_d^{\text{fid}}$  for the four different pairs of datasets resulting from forecasts of gravitational wave experiments (ET and LISA) and baryon acoustic oscillation surveys (DESI and Euclid).

For the different GW and BAO surveys, we implement the respective likelihood functions in `cobaya` [64]<sup>16</sup> and perform a Background-only MCMC analysis. Specifically, we leave  $H_0$  and  $\Omega_c h^2$  free to vary within flat ranges  $H_0 \in [20, 100]$  km/s/Mpc and  $\Omega_c h^2 \in [0.001, 0.99]$ . Instead, we assume a BBN prior  $\Omega_b h^2 = \mathcal{G}(0.0224, 0.0001)$ , and fix the following parameters to their best-fit values:

$\log(10^{10} A_s) = 3.0447$ ,  $n_s = 0.9659$ , and  $\tau = 0.0543$ .

The 1D posterior distribution functions and the 2D marginalized probability contours for the parameters of interest in our tests, obtained through MCMC analysis, are shown in Fig. 6. As is clear from the figures, the fiducial values are always recovered well within the 68% confidence level interval.

<sup>16</sup> <https://github.com/CobayaSampler/cobaya>

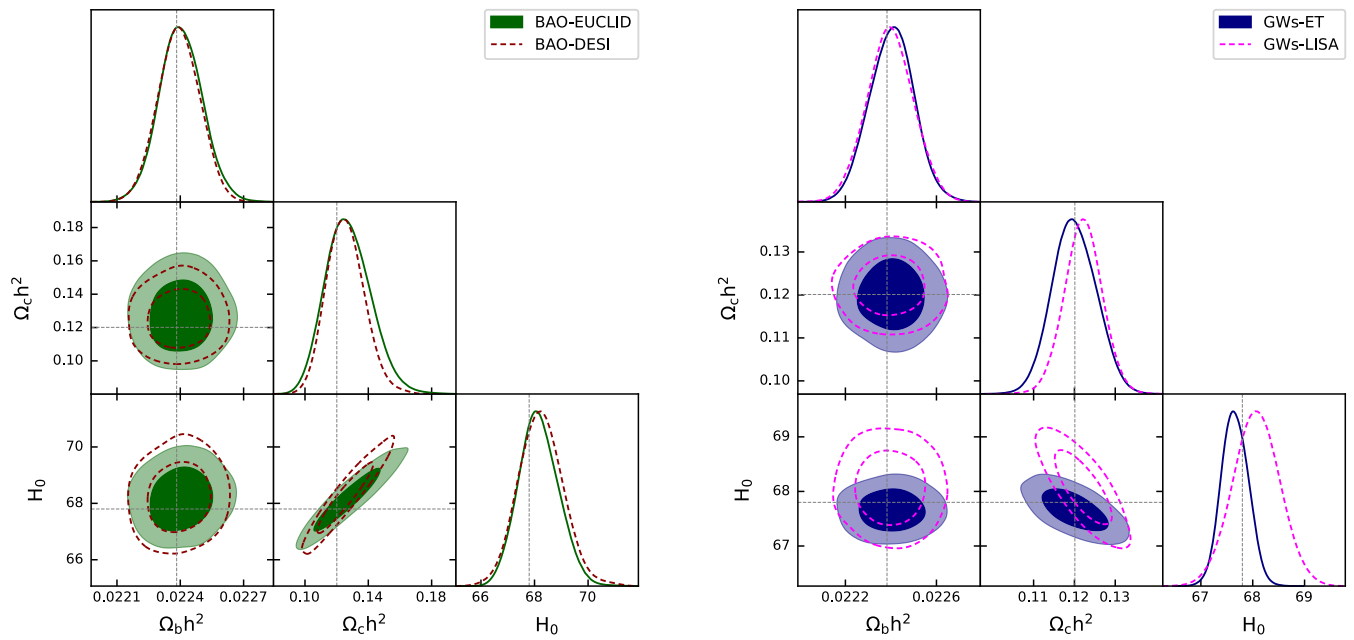


Figure 6. *Left panel:* 1D posterior distribution functions and the 2D marginalized probability contours for the parameters of interest in our tests, obtained through MCMC analysis of the DESI and Euclid BAO mock data. *Right panel:* 1D posterior distribution functions and the 2D marginalized probability contours for the same parameters obtained through MCMC analysis of the ET and LISA GW mock data.